AIAA 2004-1222

AIAA 04-1222

Laser Absorption Spectroscopy in Inductive Plasma Generator Flows

Makoto Matsui[1], Georg Herdrich[2], Monika Auweter-Kurtz[3] , and Kimya Komurasaki[4]

[1,4]Department of Advanced Energy, University of Tokyo,
Hongo 7-3-1, Bunkyo, Tokyo 113-0033, Japan

[2,3]Institut für Raumfahrtsysteme (IRS), Universität Stuttgart
Pfaffenwaldring 31, D-70550 Stuttgart, Germany

Abstract

Inductive Plasma Generator developed at the Institut für Raumfahrtsysteme (IRS) was used to produce high enthalpy pure oxygen plumes. Translational temperature was obtained by laser absorption spectroscopy using an absorption line from meta-stable atomic oxygen at 777.19nm. As a result, emission and absorption signals were found to fluctuate at 300Hz. Maximum translational temperature was 6,700K on the centerline and 4000K at the edge of the plume. Then, the spatially averaged static enthalpy and kinetic enthalpy estimated by measured temperature and corresponding frozen loss calculated under thermo-chemical equilibrium were 6.5MJ/kg 5.5MJ/kg and 15.5MJ/kg, respectively. Then, the total enthalpy was estimated to be 27.5MJ/kg. This value agrees with input enthalpy of 30MJ/kg.

1. Introduction

For developments of Thermal Protection Systems, it is necessary to simulate entry/re-entry conditions by ground test facilities. Arc-heaters are widely used to generate such high enthalpy flows for their long operational time and high input power [1~3].

However, these flows are polluted by their electrode erosions, which have adverse affects on surface catalytic research of TPS materials. Therefore, an electrode-less, Inductive Plasma Generator has been developed at IRS in order to generate metallic particle free plasma flows. The plasma in front of a probe is expected that unwanted chemical reactions due to the electrode erosions aren't present and ideal experimental conditions for the catalytic research can be produced.

The IPG has another advantage that even reactive gases, CO_2, O_2 can be used because of the electrode-less power input mechanism. Hence, Mars or Venus entry conditions can be simulated and influence of a single gas component for catalytic activity of TPS materials can be investigated [4,5].

In TPS research, heat flux measurements have been actively conducted to evaluate the catalytic effect of TPS surfaces [6,7]. However, enthalpy of the flow is difficult to be estimated from the measured heat flux due to the complex catalytic interactions [8,9].

In this study, translational temperature was obtained by laser absorption spectroscopy using an absorption line from meta-stable atomic oxygen at 777.19nm. Then, combining measured static enthalpy and kinetic enthalpy with frozen loss calculated under thermo-chemical equilibrium, enthalpy of the flow was estimated and compared with input enthalpy.

2. Measurement Method

2.1 Temperature measurement

Absorption profile is broadened by various physical mechanisms, and is expressed by a convolution of the Lorentz and the Gauss distribution [10]. Since, in our experimental conditions, Doppler broadening is dominant and other broadenings such as natural, pressure and Stark one are all neglected, the absorption profile $k(\nu)$ at the frequency ν is approximated to be Gauss distribution expressed as,

$$k(\nu) = \frac{2K}{\Delta\nu_D}\sqrt{\frac{\ln 2}{\pi}}\exp\left[-\ln 2\left\{\frac{2(\nu-\nu_0)}{\Delta\nu_D}\right\}^2\right]. \quad (1)$$

Here, ν_0 is the center absorption frequency and K is the integrated absorption coefficient. Doppler broadening $\Delta\nu_D$ is the statistical one originating from thermal motion of the particle and related to the translational temperature expressed as,

$$\Delta\nu_D = \frac{\sqrt{8R\ln 2}}{\lambda_0}\sqrt{\frac{T}{M}}. \quad (2)$$

[1]Graduate student, Student Member AIAA
[2]Research engineer
[3]Professor, Senior Member AIAA
[4]Associate Professor, Senior Member AIAA

In this study, an absorption line from meta-stable state 777.19nm was targeted. An energy diagram of this line is shown in Fig.1.

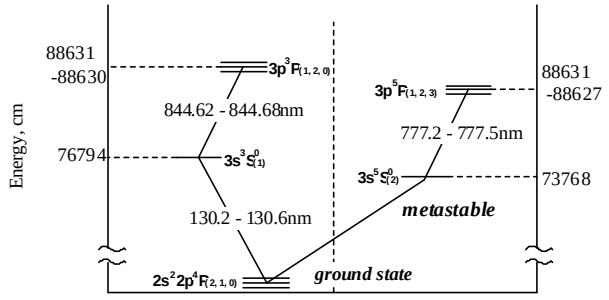

Fig.1 Energy diagram of atomic oxygen

2.2 Absorption saturation

In our previous research, influence of laser intensity on translational temperature measurement was investigated [11]. The relationship between normalized laser intensity by saturation intensity I_{sat} and estimated translational temperature in argon glow discharge plasma is shown in Fig.2, where the saturation intensity is defined as follows.

$$I_{\mathrm{sat}} = \frac{2\pi^2 h \nu^3 \Delta \nu_{\mathrm{L}}}{\phi c^2} \tag{3}$$

$$\phi = \frac{A_{ji}}{A_{ji} + Q} \tag{4}$$

Here, h is the Planck's constant, c is the velocity of light, $\Delta\nu_L$ is the Lorentzian line broadening, A is the Einstein coefficient and Q is the quenching rate. As seen in this figure, in order to obtain accurate translational temperature, normalized laser intensity should be smaller than 0.1.

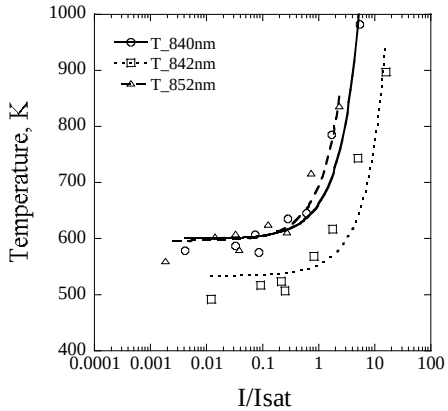

Fig.2 Relationship between normalized laser intensity and estimated translational temperature

3. Experimental Apparatus

3.1 Inductive Plasma Generator (IPG)

The schematic of IPG is shown in Fig. 3. IPG consists of gas injection and plasma production parts. Due to the variation of gas injection angle, stable plasma can be produced for various gases. The plasma production part is a quartz tube surrounded by a water-cooled induction coil. From a Meissner type resonant circuit, maximum power of 130kW can be supplied to the induction coil. The total length of IPG is about 0.35 m, its diameter about 0.08m. More details about IPG are described in references [12].

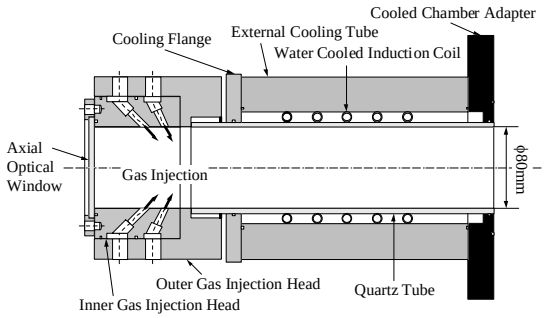

Fig.3 Schematic of IPG

3.2 Optical system

Figures 4 to 6 show a schematic and photographs of an optical system used in this research. A tunable diode-laser with an external cavity (Velocity Model 6300, New Focus) was used as a laser oscillator. The line width of the laser was smaller than 300kHz. The modulation frequency and width were 1 Hz and 30GHz, respectively. The laser intensity was 0.014mW/mm^2 and I/I_{sat} defined in Eq.(3) was 0.08. This value is enough small to avoid absorption saturation described in the section 2.2. The optical isolator was used to prevent the reflected laser beam from returning into the external cavity. The laser beam was divided into three beams by beam splitters. The first beam was directly detected by a photo-detector as a reference signal. The second was detected by an ethalon, whose free spectral range is 1GHz. The third was lead to the chamber window through a multimode optical fiber. The fiber output was mounted on a one-dimensional traverse stage to scan the plume in radial directions (see Fig.6). At the other side window, a parabola mirror was set and the laser beam can be detected without synchronizing the detector position with the laser scan. Spatial resolution was about 3mm.

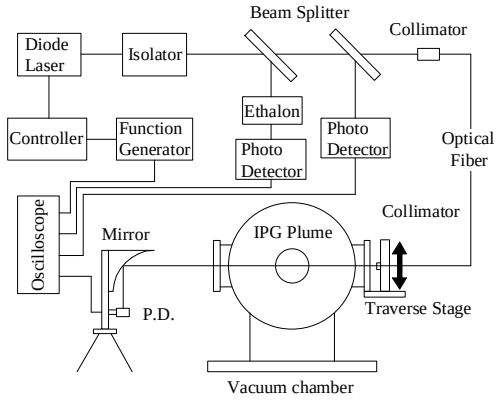

Fig.4 Optical system

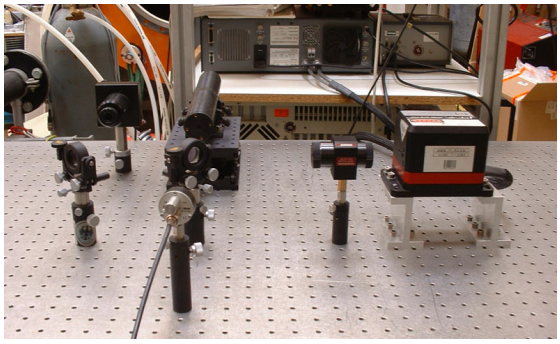

Fig.5 Photograph of optical system

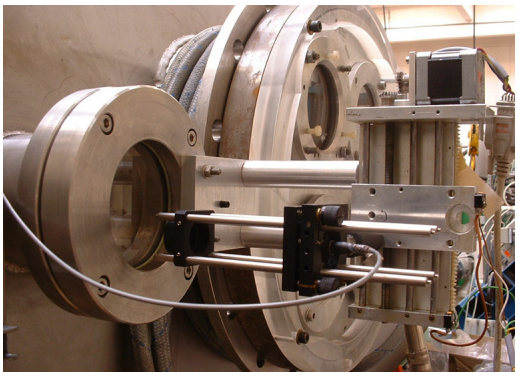

Fig.6 Photograph of laser collimate system with taraverse statge

3.3 Test conditions

Case 1 The ambient pressure was 30Pa. The oxygen mass flow rate was 4g/s, the anode input power was 110kW and the time averaged specific enthalpy was 12.5MJ/kg. The measurement plane was 130mm from the generator exit. A photograph of the plume under this condition was shown in Fig.7.

Case 2 The ambient pressure, mass flow rate were the same as in Case 1 and the anode input power was 124kW and the averaged specific enthalpy was 18.8MJ/kg. The measurement point was only 130mm only on the centerline from the generator exit, because this is the maximum input power and long operation is difficult for safety reason.

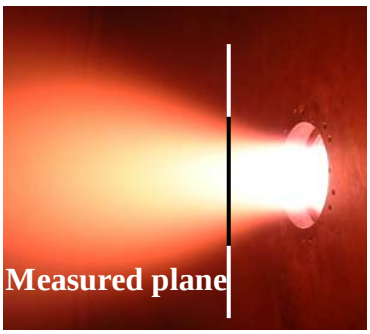

Fig.7 A photograph of IPG3 Oxygen plasma plume

4 Experimental Results

4.1 Power oscillation and emission signal

Figure 8 shows an effective plasma power characteristic curve estimated from the current characteristic of the induction coil. The averaged effective plasma power measured by a calorimeter is 50kW. As seen in this figure, in addition to the resonant oscillation, the plasma power fluctuates at the frequency of 300Hz. Then, there are two power modes: high power mode P_{high} is about 120kW and fluctuated at 300Hz, and low power mode P_{low} is about 40kW (see Fig.8). Then, the specific enthalpy was 30MJ/kg in high power mode and 10MJ/kg in low power mode, respectively.

Plasma emission signals detected by a photo detector in Cases 1 and 2 are shown in Figs.9, 10, respectively. Both emission signals also fluctuate at 300Hz. Although emission signal in both modes of Case 2 is always present (see Fig.10), in Case 1 no emission can be detected around 250μs during the low power mode (see Fig.9).

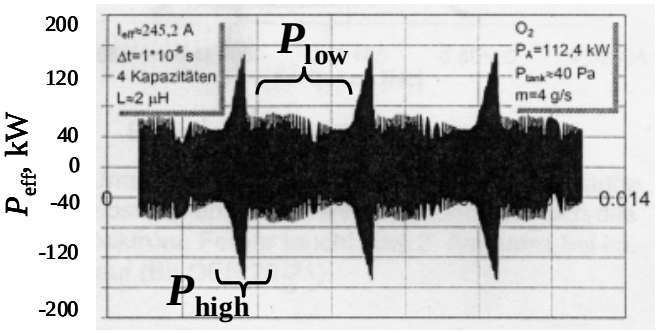

Fig.8 Current characteristic curve of induction coil

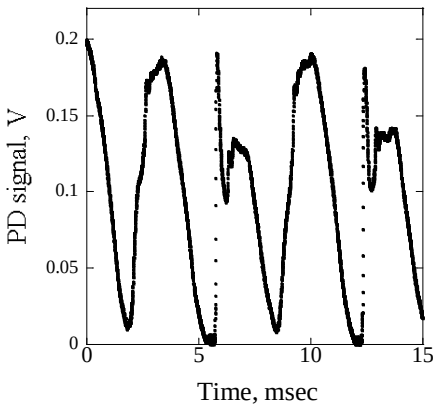

Fig.9 Plasma emission in Case 1

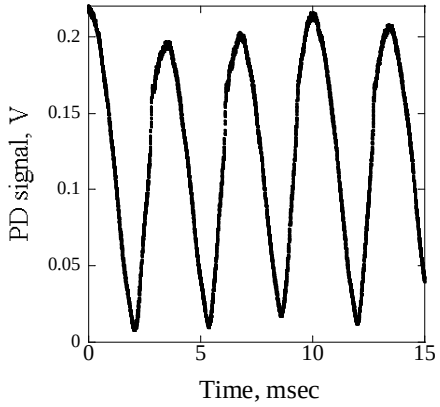

Fig.10 Plasma emission in Case 2

4.2 Absorption profiles

Case 1 A typical absorption signal in Case 1 is shown in Fig.11 along with an etalon signal. As seen in this figure, the absorption signal also fluctuates at 300Hz. Here, a maximum absorption profile defined by an envelope curve of strongest local absorption in each fluctuation is introduced. Fitting Gauss function to this profile, maximum temperature was obtained. The normalized absorption profile and Gauss fit are shown in Fig.12.

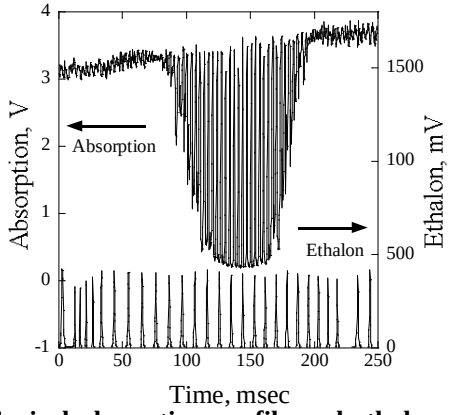

Fig.11 Typical absorption profile and ethalon signal in Case 1

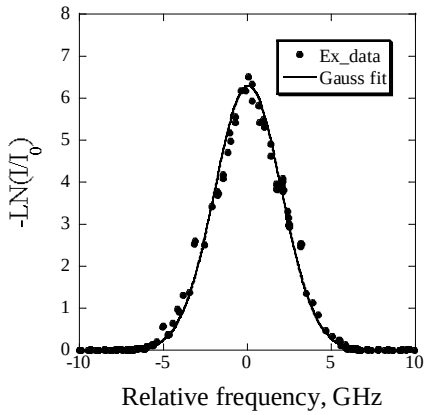

Fig.12 Maximum absorption profile and curve fittings in Case 1

Case 2 A typical absorption signal in Case 2 is shown in Fig.13 along with an etalon signal. In this case, minimum absorption profile defined by an envelope curve of weakest local absorption in each fluctuation was observed as well as the maximum one. Fitting Gauss functions to both envelope curves, maximum and minimum temperature was obtained as shown in Fig.14. As described above, in this case Abel inversion could not be applied because there wasn't enough time to obtain radial distribution. For the comparison, temperature estimated in Cases 1,2 without Abel inversion is shown in Table 1. Then, temperature variation due to the fluctuation is about 1000K. The reason that an absorption signal cannot be detected in Case 1 is low number density of meta-stable state due to the low excitation temperature.

Table 1 Temperature before Abel inversion

	T_{max}, K	T_{min}, K
Case 1	4870	-
Case 2	5273	4015

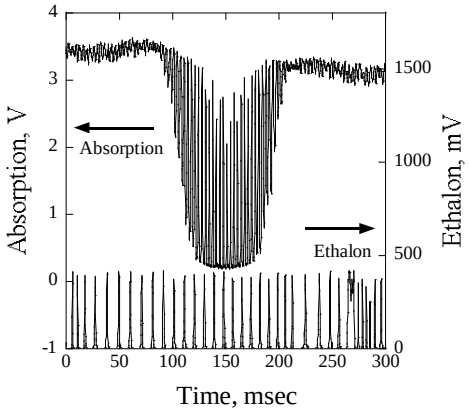

Fig.13 Typical absorption profile and ethalon signal in Case 2

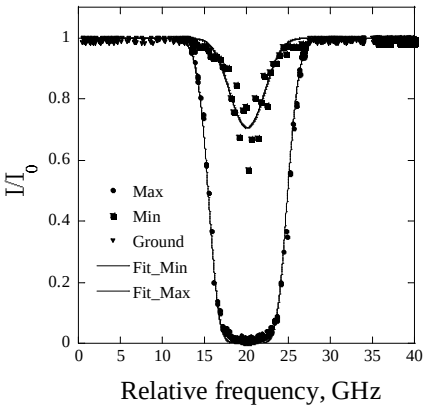

Fig.14 Maximum and minimum absorption profiles in Case 2

4.3 Maximum translational temperature

The distribution of maximum translational temperature in Case 1 is shown in Fig.15. Maximum translational temperature is ranged from 6,700K on the centerline and 4000K at the edge of the plume. Spatially averaged temperature is 5025K.

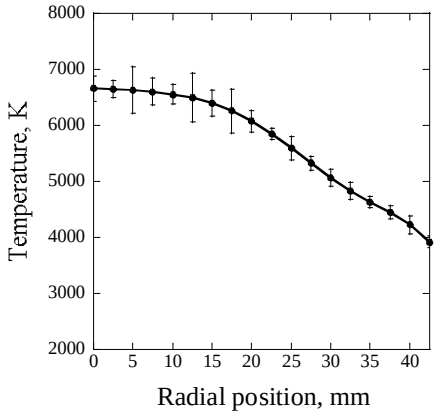

Fig.15 Maximum translational temperature distributions in Case 1

5. Discussion

5.1 Thermo-chemical equilibrium calculation

Figure 16 shows temperature, mole fraction of chemical composition and specific enthalpy calculated under thermo-chemical condition for the range from 1500K to 8500K. The specific enthalpy corresponding to the measured temperature is 22MJ/kg. Since in this calculation the flow is stagnated and flow velocity equals to zero, the frozen loss is estimated to be 15.5MJ/kg.

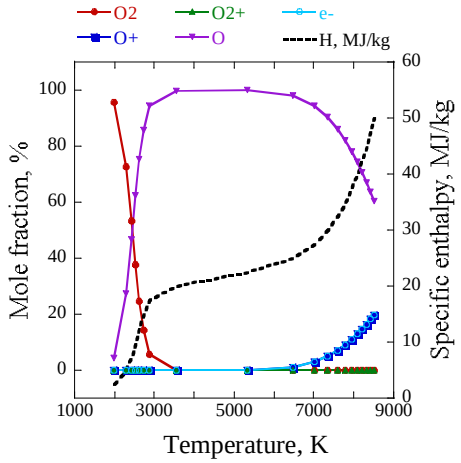

Fig.16 Temperature, specific enthalpy and mole fraction of chemical composition in the range from 1500K to 8500K (p_{amb}=30Pa)

5.2 Comparison of total and input enthalpy

Since total enthalpy of the flow is a sum of static enthalpy, kinetic enthalpy and frozen loss, the relationship between these parameters is expressed as follows.

$$H_{tot} = \frac{\int_0^{r_{max}} \rho u(h + h_{kinetic} + h_{frozen}) 2\pi r dr}{\dot{m}\pi r_{max}^2} = P/\dot{m} \quad (5)$$

Static enthalpy and kinetic enthalpy are related to translational temperature as follows.

$$h = C_p T \quad (6)$$

$$h_{kinetic} = u^2/2 = M\sqrt{\gamma RT} \quad (7)$$

Here, H_{tot} is the total enthalpy, h is the static enthalpy, $h_{kinetic}$ is the kinetic enthalpy, h_{frozen} is the enthalpy consumed for chemical reactions, u is the flow velocity, ρ is the density, r_{max} is the plume radius, P is the plasma power, $\dot{m}$ is the mass flow rate, C_p is the specific heat at constant pressure, M is the Mach number of the flow γ is the ratio of specific heats and R is gas constant.

Static enthalpy, kinetic enthalpy and frozen loss distributions estimated by measured temperature, Mach number and calculation in section 5.1 in high power mode are shown in Fig.17. The spatially averaged static and kinetic enthalpy are 6.5MJ/kg and 5.5MJ/kg, respectively. Then, the spatially averaged total enthalpy is 27.5MJ/kg. This agrees with the input enthalpy of 30MJ/kg as shown in Table2. The slight difference is thought to be due to the radiation loss.

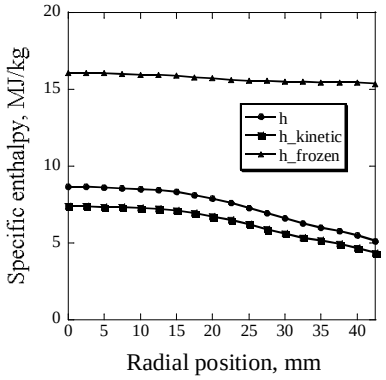

Fig.17 Static and kinetic enthalpy distribution estimated by measured temperature and Mach number

Table 2 Comparison of total and input enthalpy

	h	$h_{kinetic}$	h_{frozen}	Sum
H_{tot}	6.5MJ/kg	5.5MJ/kg	15.5kg	27.5MJ/kg
H_{input}	-	-	-	30MJ/kg

6. Summary

- Laser absorption spectroscopy was applied to the IPG plumes and translational was obtained.
- In addition to the resonance oscillation, both emission and absorption signals were found to fluctuate at the frequency of 300Hz.
- As a result, maximum translational temperature was 7,000K on the centerline and 4000K at the edge of the plume.
- The total enthalpy is estimated to be 27.5MJ/kg and agrees with the input enthalpy of 30MJ/kg.

Reference

[1] Storm, P. V. and Cappelli, M. A.: Laser-induced fluorescence measurements within an arcjet thruser nozzle, AIAA paper 95-2381, July 1995.

[2] Winter, M. W. and Auweter-Kurtz, M.: Boundary layer investigation in front of a blunt body in a subsonic air plasma flow by emission spectroscopic means, AIAA paper 98-2460, June, 1998.

[3] Salinas, I. T., Park, C., Strawa, A.W., Gopaul N. and Taunk, A.W.: Spectral Measurements in the Arc Column of an Arc-Jet Wind Tunnel, AIAA Paper 94-2595

[4] Herdrich, G., Auweter-Kurtz, M. and Kurtz, H.: New Inductively Heated Plasma Source for Reentry Simulations, Journal of Thermophysics and Heat Transfer, vol.14 pp244-249, 2000

[5] Herdrich, G., Auweter-Kurtz, M., Kurtz, H., Laux, T. and Schreiber, E.: Investigation of the Inductively Heated Plasmagenerator IPG3 Using Injection Rings of Different Geometries. AIAA 00-33547

[6] Stockle, S., Fasoulas, S., Auweter-Kurtz, M.: Heterogeneous Catalytic Recombination Reactions Including Energy Accommodation Considerations in High Enthalp Flows, AIAA paper 97-2561

[7] Laux, T., Feigl, M., Auweter-Kurtz, M., Stockle, T.: Estimation of Surface Catalytcity of PVD-Coatings by Simultaneous Heat Flux and LIF Measurements in High Enthalpy Air Flows. AIAA paper 00-2364

[8] Fay, J. A., Riddell, F. R.: Theory of Stagnation Point Heat Transfer in Dissociated Air, Journal of the Aero nautical Sciences, Vol.25, No.2, 1958

[9] Mmarvin, J.G., Pope, R.B.: Laminar Convective Heating and Ablation in the Mars Atmosphere, AIAA Journal, Mol.5, No.2, 1967

[10] Matsui, M., Komurasaki, K., Arakawa, Y.: Laser Diagnostics of Atomic Oxygen in Arc-Heater Plumes, AIAA 02-0793

[11] Matsui, M., Satoshi, O., Komurasaki, K., Arakawa, Y.: Translational Temperature Measurement of Arc-heater Pumes by a Laser Absorption Spectroscopy, AIAA 03-0587, 2003

[12] Herdrich, G., Auweter-Kurtz, M., Kurtz, H., Laux, T., and Winter, M., Operational Behavior of the Inductively Heated Plasma Source IPG3 for Re-Entry Simulations, Journal of Thermophysics and Heat Transfer, Mol.16, No.3, 2002